IEEE Access
Multidisciplinary | Rapid Review | Open Access Journal

Received September 17, 2020, accepted September 20, 2020, date of publication September 24, 2020,
date of current version October 7, 2020.

Digital Object Identifier 10.1109/ACCESS.2020.3026358

All-Dielectric Transparent Metamaterial Absorber With Encapsulated Water

QINGMIN WANG[1,2], KE BI[2], (Member, IEEE), AND SUNGJOON LIM[3], (Member, IEEE)

[1]Hebei Key Laboratory of Electromagnetic Environmental Effects and Information Processing, School of Information Science and Technology, Shijiazhuang Tiedao University, Shijiazhuang 050043, China
[2]State Key Laboratory of Information Photonics and Optical Communications, School of Science, Beijing University of Posts and Telecommunications, Beijing 100876, China
[3]School of Electrical and Electronics Engineering, Chung-Ang University, Seoul 06974, South Korea

Corresponding author: Sungjoon Lim (sungjoon@cau.ac.kr)

This work was supported in part by the National Research Foundation of Korea (NRF) funded by the Korean Government (MSIP) under Grant 2017R1A2B3003856, in part by the National Natural Science Foundation of China under Grant 61672108 and Grant 61976025, and in part by the Ph.D. Short Term Abroad Exchange Program of the Beijing University of Posts and Telecommunications (BUPT), China.

ABSTRACT An all-dielectric transparent metamaterial absorber with encapsulated water is demonstrated in this paper. Because the proposed absorber is realized using only water and polydimethylsiloxane (PDMS) without any conductive patterns, optical transparency is achieved. In addition, the high dielectric loss of water renders it a good candidate for an electromagnetic absorber. The absorptivity is increased by encapsulating the water within the PDMS, and the absorptivity of the proposed absorber is numerically compared with that of the PDMS and water with the same size. When the proposed absorber is realized using two layers, 92.5% absorptivity is achieved at 10.8 GHz, and the absorptivity exceeds 90% in the range of 10.45 to 11.20 GHz, which corresponds to 6.9% bandwidth. Therefore, the proposed absorber has advantages of high transparency, low cost, wide absorption bandwidth, and eco-friendly fabrication.

INDEX TERMS All-dielectric, transparent metamaterial, encapsulated water, electromagnetic absorber.

I. INTRODUCTION

In the past several years, metamaterial absorbers have rapidly developed owing to their ability to customize the frequency-dependent absorptivity and emissivity and to provide a more diversified absorption performance. Metamaterial absorbers have many potential applications for energy harvesting, radar stealth, and electromagnetic compatibility [1]–[6], Most of the present metamaterial absorbers have three-layer configurations consisting of a dielectric spacer and two separating metal layers. One or both of the metal layers are made of periodically patterned resonators [7]–[13]. The three-layer structure concentrates the incident electromagnetic waves between the two metal layers and then dissipates them as heat at the resonant frequency of the metamaterial [14], [15]. By designing a suitable metamaterial structure, the metal–dielectric–metal three-layer metamaterial absorbers can help control the electric and magnetic resonances independently to allow perfect matching with free space as well as complete energy absorption. However, the metal–dielectric–metal three-layer absorbers employ high conductivity metals to produce high-Q inductive and capacitive resonances for manipulating the effective permittivity and permeability, which cause metal ohmic damping that limit the applications of the absorbers [16], [17]. In addition, in the case of the metal absorbers, saturation of the magnetic response resulting from the electron kinetic induction of metal near the plasmon resonance frequency further limits the application of metal absorbers at high frequencies [18]–[20].

To overcome these limitations, a strategy of replacing the metallic structure with dielectric counterparts has been evaluated [21], [22]. Dielectric metamaterial absorbers with simple dielectric particles as the absorbed elements can produce electric or magnetic resonances in response to complete resonant absorption, which effectively eliminates metal ohmic loss and improves the operating frequency [23]–[25]. However, most of the proposed dielectric metamaterial absorbers still use metal substrates to achieve full electromagnetic shielding, which inevitably causes problems such as electromagnetic interference [26]–[28].

In this paper, we propose an all-dielectric transparent metamaterial absorber with encapsulated water. The proposed metamaterial absorber is constructed using dielectric materials such as water and polydimethylsiloxane (PDMS) without

The associate editor coordinating the review of this manuscript and approving it for publication was Luyu Zhao.

conductors. Water is a good material for transparent absorber applications because of its high permittivity, high tangential loss, and transparency [29]–[32]. The PDMS material is used to encapsulate the water. The proposed absorber thus has the advantages of high transparency, low cost, wide absorption bandwidth, and eco-friendly fabrication, which have great applications for the window of electromagnetic compatible structures and stealth devices.

II. THEORETICAL ANALYSIS

When electromagnetic waves are normally incident on a water-encapsulated metamaterial absorber, the equivalent complex impedance ($Z(\omega)$) can be used to characterize the absorption performance [33]–[35] as follows:

$$Z = \sqrt{\frac{(1+S_{11})^2 - S_{21}^2}{(1-S_{11})^2 - S_{21}^2}} \tag{1}$$

Here, Z is a pre-condition of perfect absorption, S_{11} and S_{21} are the reflection and transmission coefficients, respectively. When $Z(\omega) = \sqrt{\mu(\omega)/\varepsilon(\omega)} = 1$, the absorber can match the free space, and the magnetic and electric fields can be completely absorbed.

The effective permittivity ε and effective permeability μ of the encapsulated water within the PDMS metamaterial can be expressed as [36]

$$\varepsilon = \varepsilon_1 \left(1 + \frac{3v}{\frac{F(\theta)+2K_e}{F(\theta)-K_e} - v}\right) \tag{2}$$

$$\mu = \left(1 + \frac{3v}{\frac{F(\theta)+2K_m}{F(\theta)-K_m} - v}\right) \tag{3}$$

where $K_e = \varepsilon_{1/}\varepsilon_2$, $K_m = \mu_{1/}\mu_2$. $F(\theta)$ is the resonance function and v is the volume fraction of the water unit cell. ε_2 and μ_2 are the permittivity and permeability of water, and ε_1 and μ_1 are the permittivity and permeability of the embedded PDMS matrix, respectively.

III. DESIGN

The graphical illustration of the proposed transparent metamaterial absorber is shown in Fig. 1(a), and Fig. 1(b) describes the fabrication process and the unit cell of the absorber. The container for the water unit cell consists of a PDMS cap and a PDMS cavity, and the water particles are periodically encapsulated in the PDMS container. The sample is fabricated by the following steps. Firstly, a mold has been made according to the sizes of the waveguide and cavity. Secondly, the liquid PDMS was injected into the cavity. After the PDMS is formed, the PDMS was taken out from the mold and the cavity was sealed. Finally, the water is injected into the cavity by a syringe. The geometric parameters of the water unit cell are shown in Fig. 1(b). The water unit cell is a cuboid particle and has dimensions of $6.5 \times 6.5 \times 5.0$ mm^3 ($a \times a \times d$ mm^3). The side length and thickness of the encapsulated water is represented by a and d. The lattice period of the water-encapsulated metamaterial absorber is $p = 12$ mm, and the thickness of the PDMS container is $t = 9.0$ mm. The commercial CST Microwave software is used to optimize the dimensions of the water-encapsulated metamaterial absorber to obtain high absorptivity. In the simulation, the wave source is plane wave. The boundary condition of z direction is open (add space), the boundary conditions of x and y direction are unit cell, which are period boundaries. The incoming electromagnetic waves propagate along the z axis. The high dielectric loss of the water can produce good impedance matching of the water-encapsulated metamaterial absorber with free space and also perfect absorption.

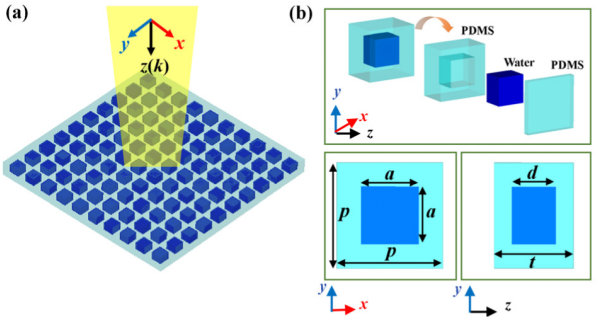

FIGURE 1. (a) Graphical illustration of the proposed metamaterial absorber. (b) Unit cell of the proposed metamaterial absorber with encapsulated water.

The Debye model is used to characterize the dielectric properties of pure water, as shown in Fig. 2(a) [37]. The real part of the permittivity of water tends to decrease from 67.2 to 56.1 in the frequency range of 8–12 GHz, behaving as an obvious frequency-dependent feature. This frequency-dependent feature may help overcome problems such as narrow absorption bands induced by varying electrical sizes of the dielectric absorber with frequency. In contrast, the corresponding loss tangent exhibits an increasing trend and maintains a high value within the operating frequency range, which benefits high absorptivity. PDMS is chosen as the material for the water container because of its low thermal conductance and easy fabrication. In simulations, the supporter was set as a material without influence on the electromagnetic waves. The dielectric constant and loss of the PDMS are influenced by the electromagnetic waves frequency. In order to investigate the absorption of water unit cell, the influence of the PDMS are subtracted in simulation and experiment. As shown in Fig. 2(b), the simulated absorptivity of supporter for the same size as the water-encapsulated metamaterial absorber is approximately 0 for 8-12 GHz and is marked in black line. The absorptivity of water for the same sized cell is marked by the red line and is less than 40% because water has a strong frequency-dispersive permittivity. However, the absorptivity is still weak because the large permittivity of water causes impedance mismatches. The absorptivity of the water-encapsulated metamaterial absorber with periodically encapsulated water within the PDMS substrate, as marked in the blue line, is 50% to 70% at 8-12 GHz. Because impedance mismatches can be

ameliorated by the periodically encapsulated water structure with effective permittivity, the water-encapsulated metamaterial absorber in the PDMS substrate has higher absorptivity than water alone. In addition, because the high absorptivity of the water-encapsulated metamaterial absorber is mainly a result of the artificially designed structure, customizing the effective permittivity of the absorber can enable improvements in the absorbed bandwidth and efficiency.

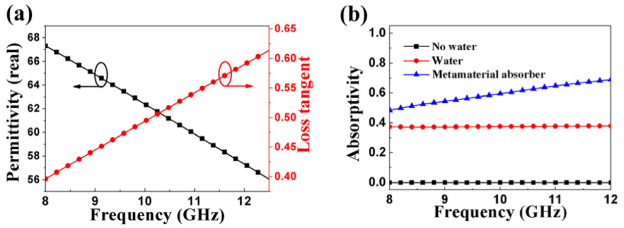

FIGURE 2. (a) Plot of the fitted permittivity and loss tangent of water from Debye model versus frequency. (b) Simulated absorptivity of the water-encapsulated metamaterial absorber; this absorptivity is compared with the absorptivity of the PDMS and water of the same size.

To optimize the dimensions of the water-encapsulated metamaterial absorber unit cell, three main parameters were simulated and evaluated for high absorptivity. The absorptivity of the water-encapsulated metamaterial absorber was obtained using the relation

$$A(\omega) = 1 - R(\omega) - T(\omega) = 1|S_{11}|^2 - |S_{21}|^2 \quad (4)$$

If the S parameters include the co-polarized electromagnetic waves and cross-polarized electromagnetic waves, the S parameters can be expressed as: [38]–[40]

$$|S_{11}|^2 = |S_{11,xx}|^2 + |S_{11,xy}|^2 \quad (5)$$

$$|S_{21}|^2 = |S_{21,xx}|^2 + |S_{21,xy}|^2 \quad (6)$$

The absorptivity of the water-encapsulated metamaterials can be expressed as:

$$A(\omega) = 1 - |S_{11,xx}|^2 - |S_{11,xy}|^2 - |S_{21,xx}|^2 - |S_{21,xy}|^2 \quad (7)$$

Because the proposed water-based absorber does not produce cross-polarized electromagnetic waves, the Eq. 4 is still used to calculate the absorptivities. To obtain absorptivity values as close to unity as possible, both reflectivity $R(\omega)$ and transmissivity $T(\omega)$ should be minimized at the resonant frequency. The effect of water unit cell size on the absorptivity of the water-encapsulated absorber was then investigated. The thickness of the water layer is of great importance for the absorption performance. Figure 3(a) shows the absorptivity and Fig. 3(b) shows the corresponding extracted maximum absorptivity. When the other dimensions are fixed, the maximum absorptivity of the water-encapsulated absorber increases with d from 1.0 mm to 3.0 mm and then remains almost unchanged as d continues to increase. The side length a of the water layer also plays an important role in the absorptivity. Figure 3(c) shows the absorptivity of the water-encapsulated absorber for different side lengths a of the water layer, and Fig. 3(d) shows the corresponding extracted maximum absorptivity. When the other dimensions are fixed, the maximum absorptivity increases with a from 2.5 mm to 8.5 mm and then decreases thereafter. In consideration of the fabrication process and the stability of the water-encapsulated absorber, the PDMS container needs to have a thick cavity wall. Therefore, the aforementioned dimensions were chosen to fabricate the water-encapsulated absorber while maintaining the absorptivity at a relatively high value.

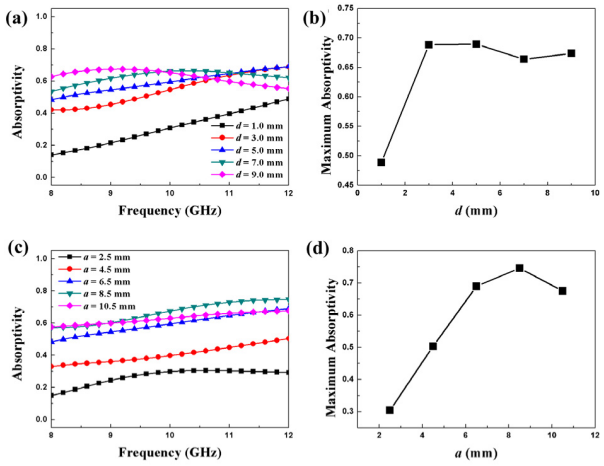

FIGURE 3. Simulated absorptivity of the proposed absorber with different (a) thickness d of water, and (c) side length a of water, and the corresponding extracted maximum absorptivities with (b) thickness d of water, and (d) side length a of water.

IV. RESULTS AND DISCUSSION

In the experiments, S_{11} and S_{21} are measured by waveguides connected to a vector network analyzer with two coaxial cables. Owing to the limitation imposed by the waveguide port size (22.86 mm×10.16 mm), as shown in Fig. 4(a), only the water-encapsulated metamaterial absorber unit cell could be fabricated and evaluated. The dimensions of the water-encapsulated absorber are the same as those of the waveguide port. As shown in Fig. 4(b), the fabricated absorber is optically transparent. Figure 4(c) shows the measured absorptivity of the absorber with single and double layers, and the simulated values are also plotted alongside for comparison. Obviously, the double layer absorber has a maximum absorptivity of 92.5% at a frequency of 10.8 GHz and a bandwidth of 0.75 GHz for over 90% absorptivity; this implies a small relative error for the simulated results for a maximum absorptivity of 95.2% at 11.6 GHz and a bandwidth exceeding 0.50 GHz for over 90% absorptivity. The measured absorptivity of the absorber with a single layer is mostly in agreement with those from the simulated results, with only a small difference between them. The differences between the simulated and measured results of the absorbers with single and double layers may be due to imperfections in the fabrication process. Another reason that may cause incomplete matching between the simulated and measured results could

be the employed waveguide, which might induce some deviations at higher frequencies.

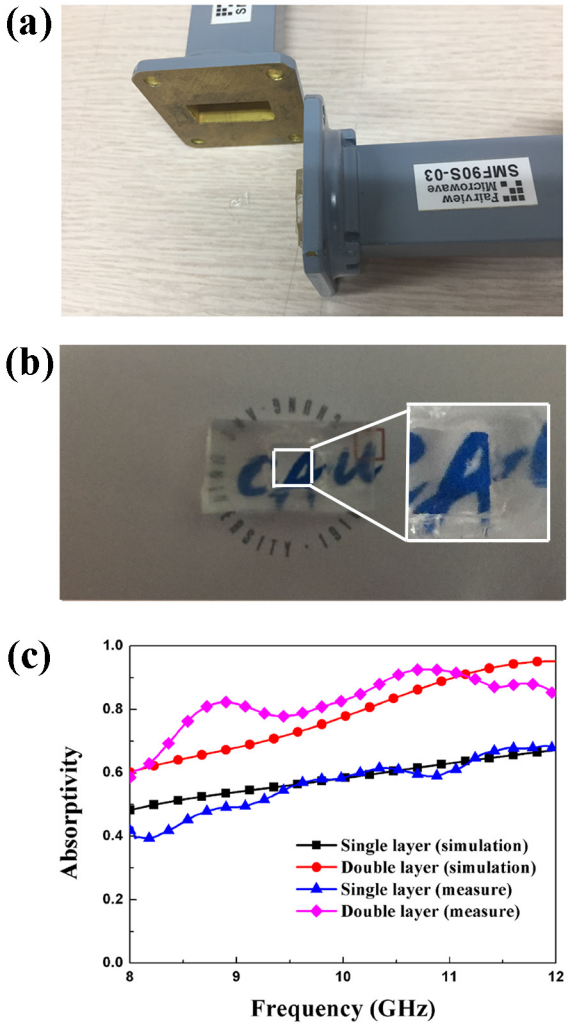

FIGURE 4. (a) Measurement setup with two rectangular waveguides with the fabricated sample inserted between them. (b) Picture of the fabricated absorber prototype. (c) Simulated and measured absorptivities of the proposed water-encapsulated metamaterial absorbers with the single and double layers.

Meanwhile, it is found that the absorptivity of the water-encapsulated metamaterial absorber is efficiently improved by increasing the number of layers. Both the simulated and measured transmissivities, reflectivities, and absorptivities of the proposed absorbers with single and double layers are presented in Fig. 5, which demonstrates that the absorptivity of the proposed absorber with the double layer is improved by reducing the reflectivity and transmissivity simultaneously [41]–[43]. Therefore, wideband and high absorptivity all-dielectric transparent metamaterial absorbers can be achieved by encapsulating water within PDMS. The discrepancy between the simulation and measurement results is observed from the double layer. This discrepancy is due to fabrication error because two layers must be manually assembled.

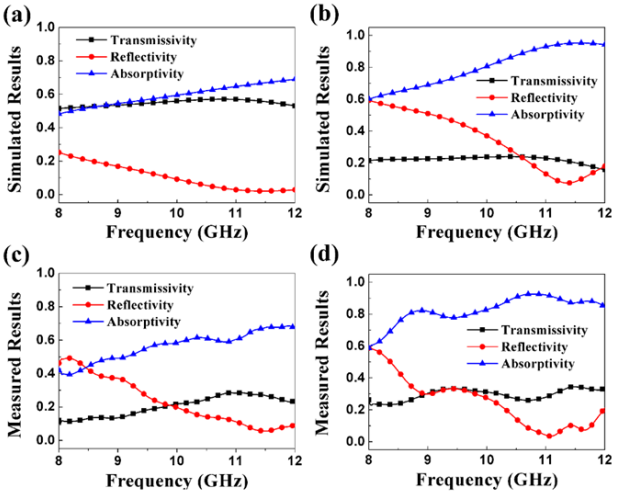

FIGURE 5. (a) Simulated transmissivity, reflectivity, and absorptivity of the proposed absorber: (a) single layer and (b) double layer. Measured transmissivity, reflectivity, and absorptivity of the proposed absorber: (c) single layer and (d) double layer.

Fig. 6 shows the simulated complex impedance which is calculated using Eq. 1. It is observed that the real part of impedance is close to 1 and the imaginary part of impedance is close to 0 at 11.6 GHz which represents the impedance matching to free space. It is the expected result because the simulated absorptivity in Fig. 5(b) is close to 100% at 11.6 GHz.

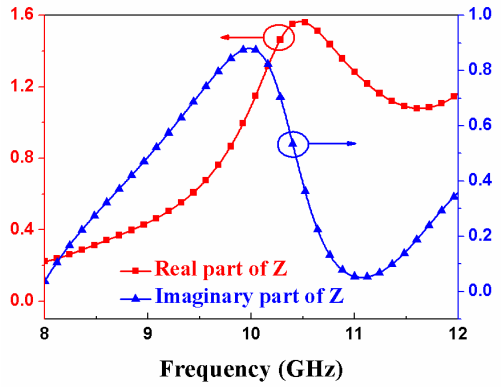

FIGURE 6. Simulated complex impedance of the proposed absorber with the double layer.

Fig. 7(a) shows the simulated absorptivities of the proposed absorber with the double layer at different incident angles θ. It is observed that the proposed absorber keeps 90% absorption bandwidth form 11.36 to 11.45 GHz when the incident angle is below 30°. When the incident angle is 30-50°, the absorptivity is higher than 90% although its bandwidth is narrower. Fig. 7(b) shows the simulated absorptivities of the proposed absorber with the double layer at different polarization angles φ under normal incidence. It is observed that the absorptivity is not changed at different polarization angle because of symmetric unit cell.

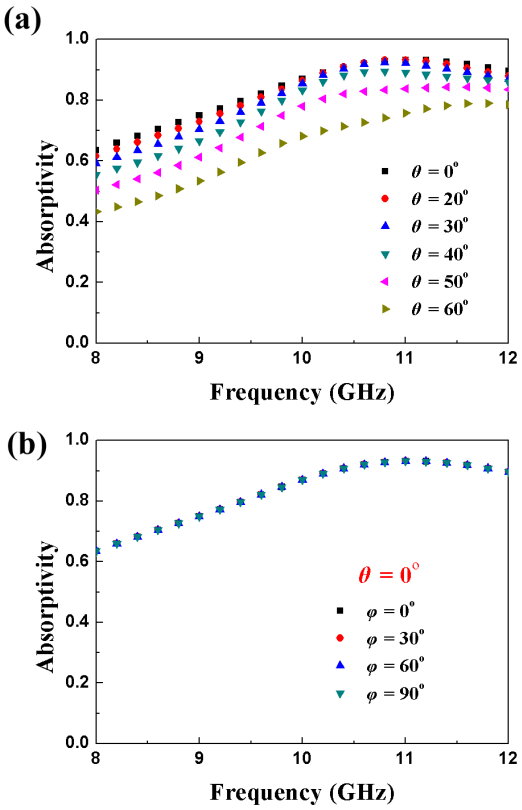

FIGURE 7. (a) Simulated absorptivities of the proposed absorber with the double layer at different incident angles θ. (b) Simulated absorptivities of the proposed absorber with the double layer at different polarization angles φ under normal incidence.

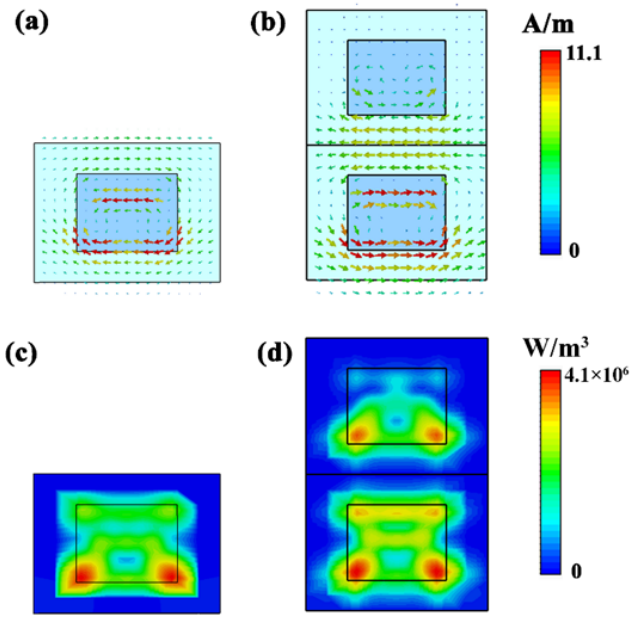

FIGURE 8. Simulated vectors of the magnetic field distributions: (a) single layer and (b) double layer. Simulated magnitudes of the power loss density distributions: (c) single layer and (d) double layer.

In order to provide a physical mechanism to demonstrate the absorption performance of the water-encapsulated metamaterial absorber, the magnetic field distributions and power loss density distributions of the absorbers with single and double layers are simulated at 11.37 GHz (Fig. 8). As shown in Fig. 8(a) and Fig. 8(b), the magnetic fields are mainly concentrated within the water unit cell. Meanwhile, the magnetic fields are mainly concentrated on the side of the incident electromagnetic waves and are relatively weaker on the opposite side because the resonance of water exists at the side of the incident electromagnetic waves. The power loss density is also concentrated within the water, which demonstrates that the absorptivity is induced by the encapsulated water. The absorptivity of the encapsulated absorber with the double layer can be improved by dissipating the electromagnetic power and reducing the reflectivity and transmissivity simultaneously. Previous water-based metamaterial absorbers require conductive patterns either on the top or bottom planes [29]–[32]. However, the proposed water-based metamaterial absorber is all-dielectric and transparent, which have great applications for the window of electromagnetic compatible structures and stealth devices.

V. CONCLUSION

We proposed an all-dielectric transparent metamaterial absorber with encapsulated water and investigated its absorptivity. The measured results show that the water-encapsulated metamaterial absorber has excellent electromagnetic energy dissipation properties. The thickness and side length of the water unit cell influence the absorptivity of the water-encapsulated metamaterial absorber unit cell. The absorptivity of the water-encapsulated absorber can thus be efficiently improved by increasing the number of layers. When the proposed absorber is realized with two layers, 92.5% absorptivity can be achieved at 10.8 GHz, and the absorptivity is higher than 90% in the range of 10.45 to 11.20 GHz, which corresponds to 6.9% bandwidth. The proposed water-encapsulated metamaterial absorber is transparent, which facilitates real-time monitoring of the shielded electromagnetic devices. The designed water-encapsulated metamaterial absorber also has the advantages of high transparency, low cost, wide absorption bandwidth, and eco-friendly fabrication, which are very suitable for modern industrial electromagnetic applications.

REFERENCES

[1] S. U. Rahman, Q. Cao, I. Gil, M. Sajjad, and Y. Wang, "Design of wide-band beamforming metasurface with alternate absorption," *IEEE Access*, vol. 8, pp. 21393–21400, 2020.

[2] Y. Cheng, H. Luo, F. Chen, and X. Mao, "Compact ultra-thin seven-band microwave metamaterial absorber based on a single resonator structure," *J. Electron. Mater.*, vol. 48, no. 6, pp. 3939–3946, Mar. 2019.

[3] Y. Cheng, B. He, J. Zhao, and R. Gong, "Ultra-thin low-frequency broadband microwave absorber based on magnetic medium and metamaterial," *J. Electron. Mater.*, vol. 46, no. 2, pp. 1293–1299, 2017.

[4] H. Luo and Y. Z. Cheng, "Ultra-thin dual-band polarization-insensitive and wide-angle perfect metamaterial absorber based on a single circular sector resonator structure," *J. Electron. Mater.*, vol. 47, no. 1, pp. 323–328, Jan. 2018.

[5] Y. Cheng, H. Luo, and F. Chen, "Broadband metamaterial microwave absorber based on asymmetric sectional resonator structures," *J. Appl. Phys.*, vol. 127, no. 21, Jun. 2020, Art. no. 214902.
[6] Q. Wang and Y. Cheng, "Compact and low-frequency broadband microwave metamaterial absorber based on meander wire structure loaded resistors," *AEU-Int. J. Electron. Commun.*, vol. 120, Jun. 2020, Art. no. 153198.
[7] G. Deng, P. Chen, J. Yang, Z. Yin, and L. Qiu, "Graphene-based tunable polarization sensitive terahertz metamaterial absorber," *Opt. Commun.*, vol. 380, pp. 101–107, Dec. 2016.
[8] F. Chen, Y. Cheng, and H. Luo, "Temperature tunable narrow-band terahertz metasurface absorber based on InSb micro-cylinder arrays for enhanced sensing application," *IEEE Access*, vol. 8, pp. 82981–82988, 2020.
[9] N. I. Landy, S. Sajuyigbe, J. J. Mock, D. R. Smith, and W. J. Padilla, "Perfect metamaterial absorber," *Phys. Rev. Lett.*, vol. 100, May 2008, Art. no. 207402.
[10] R. Yahiaoui, J. P. Guillet, F. de Miollis, and P. Mounaix, "Ultra-flexible multiband terahertz metamaterial absorber for conformal geometry applications," *Opt. Lett.*, vol. 38, no. 23, pp. 4988–4990, Dec. 2013.
[11] Y. Zhang, J. Duan, B. Zhang, W. Zhang, and W. Wang, "A flexible metamaterial absorber with four bands and two resonators," *J. Alloys Compounds*, vol. 705, pp. 262–268, May 2017.
[12] M. P. Ustunsoy and C. Sabah, "Dual-band high-frequency metamaterial absorber based on patch resonator for solar cell applications and its enhancement with graphene layers," *J. Alloys Compounds*, vol. 687, pp. 514–520, Dec. 2016.
[13] P. Rufangura and C. Sabah, "Wide-band polarization independent perfect metamaterial absorber based on concentric rings topology for solar cells application," *J. Alloys Compounds*, vol. 680, pp. 473–479, Sep. 2016.
[14] J. Liu, M. Zhu, N. Zhang, H. Zhang, Y. Zhou, S. Sun, N. Yi, S. Gao, Q. Song, and S. Xiao, "Wafer-scale metamaterials for polarization-insensitive and dual-band perfect absorption," *Nanoscale*, vol. 7, no. 45, pp. 18914–18917, 2015.
[15] W. Xu, L. Xie, and Y. Ying, "Mechanisms and applications of terahertz metamaterial sensing: A review," *Nanoscale*, vol. 9, no. 37, pp. 13864–13878, 2017, doi: 10.1039/C7NR03824K.
[16] P. Moitra, B. A. Slovick, Z. Gang Yu, S. Krishnamurthy, and J. Valentine, "Experimental demonstration of a broadband all-dielectric metamaterial perfect reflector," *Appl. Phys. Lett.*, vol. 104, no. 17, Apr. 2014, Art. no. 171102.
[17] C. L. Holloway, E. F. Kuester, J. Baker-Jarvis, and P. Kabos, "A double negative (DNG) composite medium composed of magnetodielectric spherical particles embedded in a matrix," *IEEE Trans. Antennas Propag.*, vol. 51, no. 10, pp. 2596–2603, Oct. 2003.
[18] K. Vynck, D. Felbacq, E. Centeno, A. I. Căbuz, D. Cassagne, and B. Guizal, "All-dielectric rod-type metamaterials at optical frequencies," *Phys. Rev. Lett.*, vol. 102, no. 13, Mar. 2009, Art. no. 133901.
[19] H. Su, J. Li, and L. Xia, "A novel temperature controlled broadband metamaterial absorber for THz applications," *IEEE Access*, vol. 7, pp. 161255–161263, 2019.
[20] A. B. Evlyukhin, C. Reinhardt, A. Seidel, B. S. Luk'yanchuk, and B. N. Chichkov, "Optical response features of Si-nanoparticle arrays," *Phys. Rev. B, Condens. Matter*, vol. 82, no. 4, Jul. 2010, Art. no. 045404.
[21] X. Liu, C. Lan, K. Bi, B. Li, Q. Zhao, and J. Zhou, "Dual band metamaterial perfect absorber based on mie resonances," *Appl. Phys. Lett.*, vol. 109, no. 6, Aug. 2016, Art. no. 062902.
[22] X. Liu, Q. Zhao, C. Lan, and J. Zhou, "Isotropic Mie resonance-based metamaterial perfect absorber," *Appl. Phys. Lett.*, vol. 103, no. 3, Jul. 2013, Art. no. 031910.
[23] Q. Qian, T. Sun, Y. Yan, and C. Wang, "Large-area wide-incident-angle metasurface perfect absorber in total visible band based on coupled Mie resonances," *Adv. Opt. Mater.*, vol. 5, no. 13, Jul. 2017, Art. no. 1700064.
[24] F. Zhang, S. Feng, K. Qiu, Z. Liu, Y. Fan, W. Zhang, Q. Zhao, and J. Zhou, "Mechanically stretchable and tunable metamaterial absorber," *Appl. Phys. Lett.*, vol. 106, no. 9, Mar. 2015, Art. no. 091907.
[25] J.-S. Kang, J.-H. Kim, K. Y. Kang, D. H. Yoon, and S. W. Park, "Specular reflectance measurements of dielectric plates in millimeter frequency range," *J. Electromagn. Eng. Sci.*, vol. 18, no. 2, pp. 78–87, Apr. 2018.
[26] R. Yahiaoui, K. Hanai, K. Takano, T. Nishida, F. Miyamaru, M. Nakajima, and M. Hangyo, "Trapping waves with terahertz metamaterial absorber based on isotropic Mie resonators," *Opt. Lett.*, vol. 40, no. 13, pp. 3197–3200, Jul. 2015.
[27] W. Li, C. Li, L. Lin, Y. Wang, and J. Zhang, "All-dielectric radar absorbing array metamaterial based on silicon carbide/carbon foam material," *J. Alloys Compounds*, vol. 781, pp. 883–891, Apr. 2019.
[28] J.-Y. Myung and S.-W. Yun, "Design of a triple-mode bandpass filter using a closed loop resonator," *J. Electromagn. Eng. Sci.*, vol. 17, no. 2, pp. 86–90, 2017.
[29] D. J. Gogoi and N. S. Bhattacharyya, "Embedded dielectric water 'atom' array for broadband microwave absorber based on Mie resonance," *J. Appl. Phys.*, vol. 122, no. 17, Nov. 2017, Art. no. 175106.
[30] H. Zhang, F. Ling, H. Wang, Y. Zhang, and B. Zhang, "A water hybrid graphene metamaterial absorber with broadband absorption," *Opt. Commun.*, vol. 463, Jan. 2020, Art. no. 125394.
[31] J. Xie, S. Quader, F. Xiao, C. He, X. Liang, J. Geng, R. Jin, W. Zhu, and I. D. Rukhlenko, "Truly all-dielectric ultrabroadband metamaterial absorber: Water-based and ground-free," *IEEE Antennas Wireless Propag. Lett.*, vol. 18, no. 3, pp. 536–540, Mar. 2019.
[32] Q. Song, W. Zhang, P. C. Wu, W. Zhu, Z. X. Shen, P. H. J. Chong, Q. X. Liang, Z. C. Yang, Y. L. Hao, H. Cai, H. F. Zhou, Y. Gu, G. Lo, D. P. Tsai, T. Bourouina, Y. Leprince-Wang, and A. Liu, "Water-resonator-based metasurface: An ultrabroadband and near-unity absorption," *Adv. Opt. Mater.*, vol. 5, no. 8, Apr. 2017, Art. no. 1601103.
[33] Y.-Q. Pang, Y.-J. Zhou, and J. Wang, "Equivalent circuit method analysis of the influence of frequency selective surface resistance on the frequency response of metamaterial absorbers," *J. Appl. Phys.*, vol. 110, no. 2, 2011, Art. no. 023704.
[34] X. Huang, H. Yang, S. Yu, J. Wang, M. Li, and Q. Ye, "Triple-band polarization-insensitive wide-angle ultra-thin planar spiral metamaterial absorber," *J. Appl. Phys.*, vol. 113, no. 21, Jun. 2013, Art. no. 213516.
[35] H. Li, L. H. Yuan, B. Zhou, X. P. Shen, Q. Cheng, and T. J. Cui, "Ultrathin multiband gigahertz metamaterial absorbers," *J. Appl. Phys.*, vol. 110, no. 1, Jul. 2011, Art. no. 014909.
[36] Q. Wang, R. Zhou, X. Wang, Y. Guo, Y. Hao, M. Lei, and K. Bi, "Wideband terahertz absorber based on mie resonance metasurface," *AIP Adv.*, vol. 7, no. 11, Nov. 2017, Art. no. 115310.
[37] W. J. Ellison, "Permittivity of pure water, at standard atmospheric pressure, over the frequency range 0–25 THz and the temperature range 0–100 °C," *J. Phys. Chem. Reference Data*, vol. 36, no. 1, pp. 1–18, Mar. 2007.
[38] S. Li, Y. Li, H. Li, Z. Wang, C. Zhang, Z. Guo, R. Li, X. Cao, Q. Cheng, and T. Cui, "A thin self-feeding Janus metasurface for manipulating incident waves and emitting radiation waves simultaneously," *Annalen der Physik*, vol. 532, no. 5, Apr. 2020, Art. no. 2000020.
[39] S. Li, T. Cui, Y. Li, C. Zhang, R. Li, X. Cao, and Z. Guo, "Multifunctional and multiband fractal metasurface based on inter-metamolecular coupling interaction," *Adv. Theory Simul.*, vol. 2, no. 8, 2019, Art. no. 1900105.
[40] S. Li, P. X. Wu, H. X. Xu, Y. L. Zhou, X. Y. Cao, J. F. Han, C. Zhang, H. H. Yang, and Z. Zhang, "Ultra-wideband and polarization-insensitive perfect absorber using multilayer metamaterials, lumped resistors, and strong coupling effects," *Nanoscale Res. Lett.*, vol. 13, no. 1, p. 386, 2018.
[41] Q. Feng, M. Pu, C. Hu, and X. Luo, "Engineering the dispersion of metamaterial surface for broadband infrared absorption," *Opt. Lett.*, vol. 37, no. 11, pp. 2133–2135, Jun. 2012.
[42] Y. Huang, J. Luo, M. Pu, Y. Guo, Z. Zhao, X. Ma, X. Li, and X. Luo, "Catenary electromagnetics for ultra-broadband lightweight absorbers and large-scale flat antennas," *Adv. Sci.*, vol. 6, no. 7, Apr. 2019, Art. no. 1801691.
[43] Y. Guo, Y. Wang, M. Pu, Z. Zhao, X. Wu, X. Ma, C. Wang, L. Yan, and X. Luo, "Dispersion management of anisotropic metamirror for super-octave bandwidth polarization conversion," *Sci. Rep.*, vol. 5, p. 8434, Feb. 2015.

QINGMIN WANG received the B.S. degree in physics from Hebei Normal University, Shijiazhuang, China, in 2014, and the Ph.D. degree from the Beijing University of Posts and Telecommunications, Beijing, China. She is currently working with Shijiazhuang Tiedao University. Her research interests include wireless communications, metamaterials, and microwave sensors.

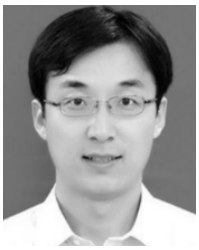

KE BI (Member, IEEE) received the Ph.D. degree from the Nanjing University of Aeronautics and Astronautics in 2012. From 2012 to 2014, he was an Assistant Researcher with Tsinghua University. He is currently an Associate Professor with the Beijing University of Posts and Telecommunications. His research interests include information functional materials and devices, and electromagnetic metamaterials and devices.

SUNGJOON LIM (Member, IEEE) received the B.S. degree in electronics engineering from Yonsei University, Seoul, South Korea, in 2002, and the M.S. and Ph.D. degrees in electrical engineering from the University of California at Los Angeles (UCLA), Los Angeles, CA, USA, in 2004 and 2006, respectively.

After a postdoctoral position at the Integrated Nanosystem Research Facility (INRF), University of California at Irvine, Irvine, CA, he joined the School of Electrical and Electronics Engineering, Chung-Ang University, Seoul, in 2007, where he is currently a Professor. He has authored or coauthored more than 250 international conferences, letters, and journal articles. His research interests include engineered electromagnetic structures (metamaterials, electromagnetic bandgap materials, and frequency selective surfaces), printed antennas, substrate integrated waveguide (SIW) components, inkjet-printed electronics, and RF MEMS applications. He is also interested in the modeling and design of microwave circuits and systems.

Prof. Lim received the Institution of Engineering and Technology (IET) Premium Award in 2009, the ETRI Journal Best Paper Award in 2014, the Best Paper Award from the International Workshop on Antenna Technology (iWAT) in 2015, and the International Symposium on Antennas and Propagation (ISAP) in 2018, and a CAU Distinguished Scholar.